The modeling and free vibration analysis of coupled plates of various types

Shuangxia Shi [1], Guoyong Jin [2], Mingfei Chen [3]

[123]College of Power and Energy Engineering, Harbin Engineering University,

Harbin, 150001, P. R. China

ABSTRACT

This paper is concerned with the modeling and free vibration analysis of coupled plates of various types, which includes T-shape plates, cross shape plates and a panel-linked double-panel structure. The in-plane vibration and bending vibration are considered in coupled structures. The vibration problems are solved using an improved Fourier series method in which the in-plane displacement and bending displacement are expressed as the superposition of a double Fourier cosine series and several supplementary functions to ensure (improve) the uniform convergence (rate) of the Fourier series expansion. The dynamic responses of the coupled plates are obtained using the Rayleigh-Ritz procedure based on the energy expressions for the coupled system. The accuracy and effectiveness of the proposed method are validated through numerical examples and comparison with results obtained by the finite element analysis.

Keywords: T-shape plates, cross shape plates, panel-linked double-panel structure

1. INTRODUCTION

The coupled plates including T-shape plates, cross shape plates and a panel-linked double-panel structure exist in various engineering occasions, such as ship hulls, aircraft cabins and building structures. The modeling and free vibration analysis of coupled plates capture the growing attentions from researchers and design engineers. This kind of problem can be solved by the finite element method (FEM), lacking of flexibility with the changing parameter in the analysis.

The analysis of vibration characteristics were investigated by researchers with the well-known numerical methods. In the existing investigations on coupled plates, considerable contributions (1-3) were made by researchers. Wang et al. (4) adopted a substructure approach to study the vibration of L-shaped plates and investigate the power flow characteristics of L- shaped plates. Bercin (5) studied the effects of in-plane vibrations the energy flow between coupled plates. Cheng et al. (6) made a research on energy transmission in a mechanically-linked double-wall structure coupled to acoustic enclosure. Chen and Jin (7) investigated the vibration behaviors of a box-type structure built up by plates. A combination of a traveling wave and modal solution was used by Kessissoglou (8) to describe the flexural and in-plane displacements functions of the plates in L-shaped plates. Cuschieri (9) used a mobility approach to investigate structural power-flow of an L-shaped plate, then Cuschieri and McCollum (10) used the mobility power flow approach to analyze in-plane and out-of-plane waves power transmission through L-plate junction. Dimitriadis and Pierce (11) proposed an analytical solution for the power exchange between strongly coupled plates under random excitation. The concept of receptance (a numerical approach) proposed by Azimi et al. (12) were used by Farag and Pan (13) to analyze effects of the coupling angle for the coupling edge, which were extended by Kim et al. (14) to investigate the interactions of transmission of bending waves in coupling conjunction for rectangular plates.

In the existing techniques, some assumptions are used. Modeling the real-life plate structures is more of practical significance. In this paper, the modified Fourier series method proposed by Li (15) is

[1] firecos@163.com
[2] guoyongjin@hrbeu.edu.cn
[3] net_easy123@163.com

applied for the modeling and the free vibration analysis for coupled plates. The Rayleigh's method is applied to calculate the coefficients of the modified Fourier series. The boundary conditions and coupling conditions can be simulated by four types boundary springs at edges and four types coupling spring at coupling conjunctions. The convergence and accuracy of the current method are proved by comparing the natural frequencies and mode shapes with the finite element analysis results. The effect of dimensional parameters and the coupling conditions are investigated.

2. THEORETICAL FORMULATIONS

2.1 Description of the models

The Analytical models for the coupled T-shape plates structure, cross shape plates structure and panel-linked double-panel structure under investigation, which are composed of elastic plates, are shown in Fig.2.1(a), (b) and (c), respectively. The geometry and the coordinate systems for these plates structure were showed in Fig. 2.1, in which, four types of uniform boundary spring are introduced to complete model the general restrained boundary condition. Similarly, along the structural conjunction, four types of uniform coupling spring, which are K_c , k_{c1} , k_{c2} and k_{c3} ,are introduced to completely model the coupling effect, and θ is the coupling angle of coupled plates structure. The displacements of the elastic plates with respect to this coordinate system are described by u , v and w in the x , y and z directions, respectively.

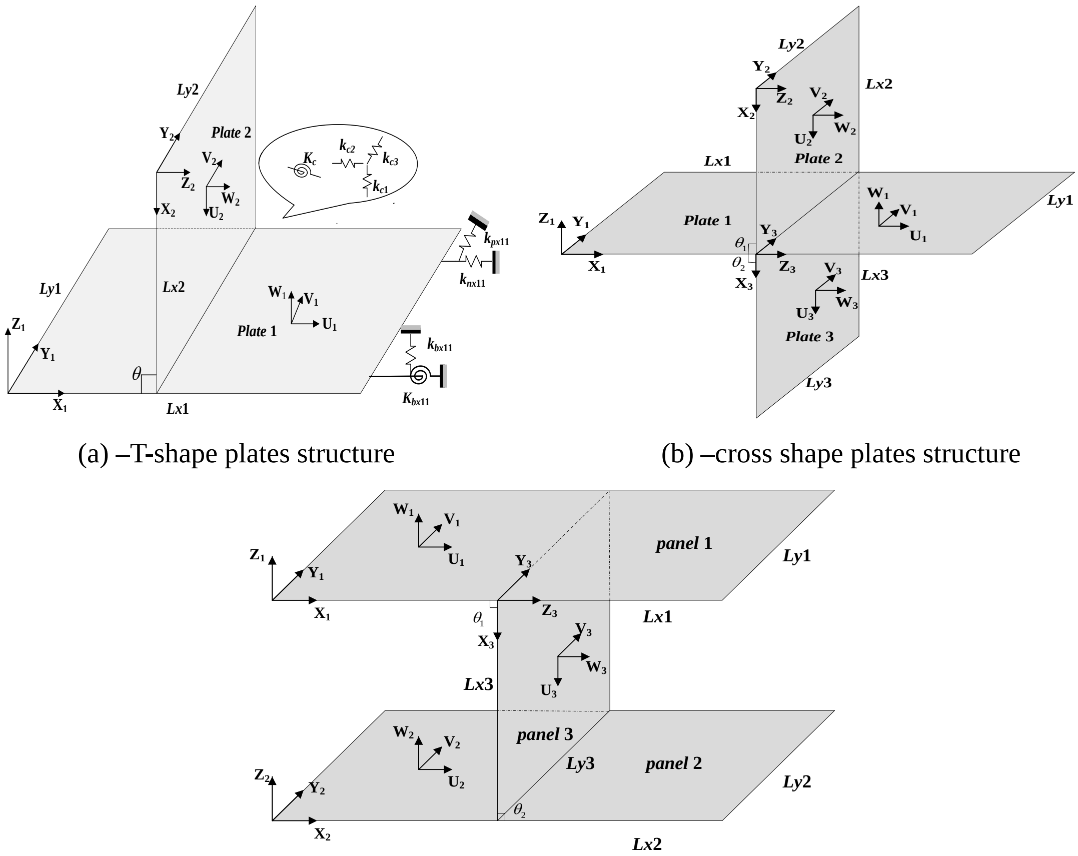

(a) –T-shape plates structure

(b) –cross shape plates structure

(c) –the panel-linked double-panel structure

Fig. 2.1 – Analytical models for coupled plates structure

2.2 Theory for bending and in-plate vibration of plates

The partial differential equations for the bending and in-plate displacement functions of plate 1 are depicted as:

$$D_1 \nabla^4 w_1\left(x_1, y_1, t\right) + \rho_1 h_1 \frac{\partial^2 w_1\left(x_1, y_1, t\right)}{\partial t^2} = 0 \tag{1}$$

$$\frac{\partial^2 u_1}{\partial x_1^{\ 2}}+\frac{1}{2}(1-\mu_1)\frac{\partial^2 u_1}{\partial y_1^{\ 2}}+\frac{1}{2}(1+\mu_1)\frac{\partial^2 v_1}{\partial x_1 \partial y_1}+\frac{1}{c_{1L}^{\ 2}}\omega^2 u_1=0 \tag{2}$$

$$\frac{\partial^2 v_1}{\partial y_1^{\ 2}}+\frac{1}{2}(1-\mu_1)\frac{\partial^2 v_1}{\partial x_1^{\ 2}}+\frac{1}{2}(1+\mu_1)\frac{\partial^2 u_1}{\partial x_1 \partial y_1}+\frac{1}{c_{1L}^{\ 2}}\omega^2 v_1=0 \tag{3}$$

where ρ_1 and h_1 , respectively, denote the mass density and the thickness of plate 1, $D_1=E_1h_1^3/(12(1-\mu_1^{\ 2}))$ is the bending rigidity of plate 1 , E_1 and μ_1 , respectively, are the Young's modulus and the Poisson ratio of the plate 1, ∇ is the Laplace operator, $c_{1L}=\sqrt{E_1/\rho_1(1-\mu_1)}$ is the p-wave speed in plate 1 structure and ω is the angular frequency of plate.

The boundary conditions for the elastic plate are:

The boundary conditions for the elastic plate considering in-plate direction are:

$$\text{on}\quad x_1=0,\qquad k_{bx10}w_1=-D_1\left(\frac{\partial^3 w_1}{\partial x_1^{\ 3}}+(2-\mu_1)\frac{\partial^3 w_1}{\partial_{x1}\partial y^2}\right), K_{bx10}\frac{\partial w_1}{\partial x_1}=D_1\left(\frac{\partial^2 w_1}{\partial x_1^{\ 2}}+\mu_1\frac{\partial^3 w_1}{\partial y_1^{\ 2}}\right) \tag{4}$$

$$k_{nx10}u_1=\frac{\partial u_1}{\partial x_1}+\mu_1\frac{\partial v_1}{\partial y_1}, k_{px10}v_1=\frac{\partial u_1}{\partial x_1}+\frac{\partial v_1}{\partial y_1}, \tag{5}$$

$$\text{on}\quad x_1=Lx1,\qquad k_{bx11}w_1=D_1\left(\frac{\partial^3 w_1}{\partial x_1^{\ 3}}+(2-\mu_1)\frac{\partial^3 w_1}{\partial x_1\partial y_1^{\ 2}}\right),\quad K_{bx11}\frac{\partial w_1}{\partial x_1}=-D_1\left(\frac{\partial^2 w_1}{\partial x_1^{\ 2}}+\mu_1\frac{\partial^3 w_1}{\partial y_1^{\ 2}}\right), \tag{6}$$

$$k_{nx11}u_1=-\frac{\partial u_1}{\partial x_1}-\mu_1\frac{\partial v_1}{\partial y1},\quad k_{px11}v_1=-\frac{\partial u_1}{\partial x_1}-\frac{\partial v_1}{\partial y_1}, \tag{7}$$

$$\text{on}\quad y_1=0,\qquad k_{by10}w_1=-D_1\left(\frac{\partial^3 w_1}{\partial y_1^{\ 3}}+(2-\mu_1)\frac{\partial^3 w_1}{\partial y_1\partial x_1^{\ 2}}\right),\quad K_{by10}\frac{\partial w_1}{\partial y_1}=D_1\left(\frac{\partial^2 w_1}{\partial y_1^{\ 2}}+\mu_1\frac{\partial^3 w_1}{\partial x_1^{\ 2}}\right), \tag{8}$$

$$k_{ny10}v_1=\frac{\partial u_1}{\partial y_1}+\mu_1\frac{\partial v_1}{\partial x_1},\quad k_{py10}u_1=\frac{\partial u_1}{\partial x_1}+\frac{\partial v_1}{\partial y_1}, \tag{9}$$

$$\text{on}\quad y_1=Ly1,\qquad k_{by11}w_1=D_1\left(\frac{\partial^3 w_1}{\partial y_1^{\ 3}}+(2-\mu_1)\frac{\partial^3 w_1}{\partial y_1\partial x_1^{\ 2}}\right),\quad K_{by11}\frac{\partial w_1}{\partial y_1}=-D_1\left(\frac{\partial^2 w_1}{\partial y_1^{\ 2}}+\mu_1\frac{\partial^3 w_1}{\partial x_1^{\ 2}}\right), \tag{10}$$

$$k_{ny11}v_1=-\frac{\partial u_1}{\partial y_1}-\mu_1\frac{\partial v_1}{\partial x_1},\quad k_{py11}u_1=-\frac{\partial u_1}{\partial x_1}-\frac{\partial v_1}{\partial y_1}, \tag{11}$$

where μ_1 is the Poisson ratio of plate 1, k and K , respectively, denote the stiffness of the translational restraining spring and the rotational restraining spring. The effect and the position are represented by the subscripts.

2.2.1 Improved series representations of the displacement functions

The displacement functions can be described by a two-dimensional Fourier cosine series method. However, discontinuity problems would be encountered in the displacement partial differential along the edges by used such a traditional Fourier cosine. To overcome the difficulty, the bending displacement function is depicted by an improved Fourier series method, which is the superposition of a two-dimensional Fourier cosine series and eight supplementary functions. Therefore, The displacement components of plate 1, w_1, u_1 and v_1 can be described as:

$$\begin{aligned} w_1(x_1,y_1)=&\sum_{m=0}^{\infty}\sum_{n=0}^{\infty}A_{1m\,n}\cos\lambda_{m\,Lx1}x_1\cos\lambda_{n\,Ly1}y_1\\ &+\sum_{m=0}^{\infty}\sum_{k=1}^{4}a_{1k\,m}\,\zeta_{k\,Ly1}(y_1)\cos\lambda_{m\,Lx1}x_1+\sum_{n=0}^{\infty}\sum_{k=1}^{4}\bar{a}_{1k\,n}\,\zeta_{k\,Lx1}(x_1)\cos\lambda_{n\,Ly1}y_1 \end{aligned} \tag{12}$$

$$\begin{aligned} u_1(x_1,y_1)=&\sum_{m=0}^{\infty}\sum_{n=0}^{\infty}B_{1m\,n}\cos\lambda_{m\,Lx1}x_1\cos\lambda_{n\,Ly1}y_1\\ &+\sum_{n=0}^{\infty}\sum_{k=1}^{2}b_{1k\,n}\,\xi_{k\,Lx1}(x_1)\cos\lambda_{n\,Ly1}y_1+\sum_{m=0}^{\infty}\sum_{k=1}^{2}\bar{b}_{1k\,m}\,\xi_{1Ly1}(y_1)\cos\lambda_{m\,Lx1}x_1 \end{aligned} \tag{13}$$

$$v_1(x_1,y_1)=\sum_{m=0}^{\infty}\sum_{n=0}^{\infty}C_{1mn}\cos\lambda_{m\,Lx1}x_1\cos\lambda_{n\,Ly1}y_1 + \sum_{n=0}^{\infty}\sum_{k=1}^{2}c_{1kn}\,\xi_{k\,Lx1}(x_1)\cos\lambda_{n\,Ly1}y_1+\sum_{m=0}^{\infty}\sum_{k=1}^{2}\bar{c}_{1km}\,\xi_{k\,Ly1}(y_1)\cos\lambda_{m\,Lx1}x_1 \tag{14}$$

where $\lambda_{m\,Lx1}=m\,\pi/Lx1,\quad \lambda_{n\,Ly1}=n\,\pi/Ly1$, n and m are all integers, describing the spatial characteristic of a particular mode, A_{1mn} , B_{1mn} , C_{1mn} , a_{1km} , $\bar{a}_{1kn}$, b_{1kn} , $\bar{b}_{1km}$, c_{1kn} and $\bar{c}_{1km}$ are the modal amplitude constants for mode (m,n), The expressions for the supplementary functions relating to x_1 are defined as:

$$\begin{cases}\zeta_{1Lx1}(x_1)=\dfrac{9Lx1}{4\pi}\sin\left(\dfrac{\pi x_1}{2Lx1}\right)-\dfrac{Lx1}{12\pi}\sin\left(\dfrac{3\pi x_1}{2Lx1}\right),\zeta_{2Lx1}(x_1)=-\dfrac{9Lx1}{4\pi}\cos\left(\dfrac{\pi x_1}{2Lx1}\right)-\dfrac{Lx1}{12\pi}\cos\left(\dfrac{3\pi x_1}{2Lx1}\right)\\ \zeta_{3Lx1}(x_1)=\dfrac{Lx1^3}{\pi^3}\sin\left(\dfrac{\pi x_1}{2Lx1}\right)-\dfrac{Lx1^3}{3\pi^3}\sin\left(\dfrac{3\pi x_1}{2Lx1}\right),\zeta_{4Lx1}(x_1)=-\dfrac{Lx1^3}{\pi^3}\cos\left(\dfrac{\pi x_1}{2Lx1}\right)-\dfrac{Lx1^3}{3\pi^3}\cos\left(\dfrac{3\pi x_1}{2Lx1}\right)\end{cases} \tag{15}$$

$$\xi_{1Lx1}(x_1)=Lx1\varsigma_{x1}(\varsigma_{x1}-1)^2,\quad \xi_{2Lx1}(x_1)=Lx1\varsigma_{x1}^2(\varsigma_{x1}-1),\quad (\varsigma_{x1}=x_1/Lx1) \tag{16}$$

It is uncomplicated to prove that

$$\zeta_{1Lx1}'(0)=\zeta_{3Lx1}'''(0)=\zeta_{2Lx1}'(Lx1)=\zeta_{4Lx1}'''(Lx1)=1, \tag{17}$$

$$\xi_{1Lx1}'(0)=\xi_{2Lx1}'(Lx1)=1, \tag{18}$$

other related partial derivative supplementary functions are zero, The expressions for the supplementary functions relating to y can be obtained by substituting x with y in Eq. (15). These conditions make related derivative of the displacement function smooth and continuous in the whole solving domain.

2.3 Solution procedure of coupled plates

In this work, the unknown expansion coefficients of the displacement functions for the coupled plates structure system are calculated by using the Rayleigh–Ritz procedure, which is actually equivalent to solve the governing equations , the boundary conditions and coupling conditions directly,

The Lagrange function for the coupled T-shape plates structure, cross shape plates structure and the panel-linked double-panel structure ,respectively, were written as:

$$L_t=U_t-T_t,\quad L_c=U_c-T_c,\quad L_g=U_g-T_g \tag{19}$$

where U and T , respectively, are the total potential energy, the total kinetic energy of coupled plates structure system, the subscript t, c and g represent the coupled T-shape plates structure, cross shape plates structure and the panel-linked double-panel structure, respectively.

$$U_t=U_{1bending}+U_{2bending}+U_{1in-pnel}+U_{2in-pnel}+U_{coupling} \tag{20}$$

$$T_t=T_{1bending}+T_{2bending}+T_{1in-pnel}+T_{2in-pnel} \tag{21}$$

$$U_c=U_{1bending}+U_{2bending}+U_{3bending}+U_{1in-pnel}+U_{2in-pnel}+U_{3in-pnel}+U^c{}_{1coupling}+U^c{}_{2coupling} \tag{22}$$

$$T_c=T_{1bending}+T_{2bending}+T_{3bending}+T_{1in-pnel}+T_{2in-pnel}+T_{3in-pnel} \tag{23}$$

$$U_g=U_{1bending}+U_{2bending}+U_{3bending}+U_{1in-pnel}+U_{2in-pnel}+U_{3in-pnel}+U^g{}_{1coupling}+U^g{}_{2coupling} \tag{24}$$

$$T_g=T_{1bending}+T_{2bending}+T_{3bending}+T_{1in-pnel}+T_{2in-pnel}+T_{3in-pnel} \tag{25}$$

where $U_{1bending}$ and $U_{1in-pnel}$, respectively, are the total bending potential energy including the total potential energy stored in the elastic springs at edges of the plate 1 and the total in-plate potential energy of the plate 1, the subscript 2 represents plate 2, $U_{coupling}$ is the total coupling potential energy of the coupled T-shape plate system.

The total potential energy and kinetic energy of the elastic plate 1 are, respectively, expressed as

$$U_{1bending}=\frac{D_1}{2}\int_0^{Ly1}\int_0^{Lx1}\left\{\left(\frac{\partial^2 w_1}{\partial x_1^{\,2}}\right)^2+\left(\frac{\partial^2 w_1}{\partial y_1^{\,2}}\right)^2+2\mu_1\frac{\partial^2 w_1}{\partial x_1^{\,2}}\frac{\partial^2 w_1}{\partial y_1^{\,2}}+2(1-\mu_1)\left(\frac{\partial^2 w_1}{\partial x_1\partial y_1}\right)^2\right\}$$
$$+\frac{1}{2}\int_0^{Ly1}\left[k_{bx10}w_1^{\,2}+K_{bx10}\left(\frac{\partial w_1}{\partial x_1}\right)^2\right]_{x_1=0}dy_1+\frac{1}{2}\int_0^{Ly1}\left[k_{bx11}w_1^{\,2}+K_{bx11}\left(\frac{\partial w_1}{\partial x_1}\right)^2\right]_{x_1=Lx1}dy_1 \quad (26)$$
$$+\frac{1}{2}\int_0^{Lx1}\left[k_{by10}w_1^{\,2}+K_{by10}\left(\frac{\partial w_1}{\partial y_1}\right)^2\right]_{y_1=0}dx_1+\frac{1}{2}\int_0^{Lx1}\left[k_{by11}w_1^{\,2}+K_{by11}\left(\frac{\partial w_1}{\partial y_1}\right)^2\right]_{y_1=Ly1}dx_1$$

$$U_{1in-panel}=\frac{G_1}{2}\int_0^{Ly1}\int_0^{Lx1}\left\{\left(\frac{\partial u_1}{\partial x_1}+\frac{\partial v_1}{\partial y_1}\right)^2-2(1-\mu_1)\frac{\partial u_1}{\partial x_1}\frac{\partial v_1}{\partial y_1}+\frac{(1-\mu_1)}{2}\left(\frac{\partial v_1}{\partial x_1}+\frac{\partial u_1}{\partial y_1}\right)^2\right\}dx_1dy_1$$
$$+\frac{1}{2}\int_0^{Ly1}\left[k_{nx10}u_1^{\,2}+k_{px10}v_1^{\,2}\right]_{x_1=0}dy_1+\frac{1}{2}\int_0^{Ly1}\left[k_{nx11}u_1^{\,2}+k_{px11}v_1^{\,2}\right]_{x_1=Lx1}dy_1 \quad (27)$$
$$+\frac{1}{2}\int_0^{Lx1}\left[k_{ny10}v_1^{\,2}+k_{py10}u_1^{\,2}\right]_{y_1=0}dx_1+\frac{1}{2}\int_0^{Lx1}\left[k_{ny11}v_1^{\,2}+k_{py11}u_1^{\,2}\right]_{y_1=Ly1}dx_1$$

$$T_{1bengding}=\frac{1}{2}\int_0^{Ly1}\int_0^{Lx1}\rho_1h_1\left(\frac{\partial w_1}{\partial t}\right)^2dx_1dy_1=\frac{1}{2}\rho_1h_1\omega^2\int_0^{Ly1}\int_0^{Lx1}w_1^{\,2}dx_1dy_1, \quad (28)$$

$$T_{1in-panel}=\frac{1}{2}\int_0^{Ly1}\int_0^{Lx1}\rho_1h_1\left[\left(\frac{\partial u_1}{\partial t}\right)^2+\left(\frac{\partial v_1}{\partial t}\right)^2\right]dx_1dy_1=\frac{1}{2}\rho_1h_1\omega^2\int_0^{Ly1}\int_0^{Lx1}\left[u_1^{\,2}+v_1^{\,2}\right]dx_1dy_1, \quad (29)$$

where $G_1=E_1\times h_1/(1-\mu_1^{\,2})$ is the tension stiffness of plate 1,the total potential energy and kinetic energy of the elastic plate 2 or plate 3 can be obtained by substituting subscript 1 with subscript 2 or subscript 3 in the above equations. Because the functions: $U^c{}_{1coupling}$, $U^c{}_{2coupling}$,$U^g{}_{1coupling}$ and $U^g{}_{2coupling}$ resemble the function $U_{coupling}$, the description of $U_{coupling}$ will be given in this paper as:

$$U_{coupling}=\frac{1}{2}\int_0^{Ly1}\left[K_c\left(\partial w_1/\partial x_1\big|_{x_1=Lx1c}-\partial w_2/\partial x_2\big|_{x_2=Lx2}\right)^2+k_{c1}\left(w_1\big|_{x_1=Lx1c}+u_2\big|_{x_2=Lx2}\right)^2\right.$$
$$\left.+k_{c2}\left(u_1\big|_{x_1=Lx1c}-w_2\big|_{x_2=Lx2}\right)^2+k_{c3}\left(v_1\big|_{x_1=Lx1c}-v_2\big|_{x_2=Lx2}\right)^2\right]dy_1 \quad (30)$$

where K_c is the rotational coupling stiffness at coupling conjunction, k_{c1} , k_{c2} and k_{c3} are the linear coupling stiffnesses at coupling conjunction in z_1-direction, x_1-direction and y_1-direction, respectively. $Lx1c$ is the coupling conjunction of plate 1.

By substituting Eqs.(12)-(14) into Eq. (19) and then applying Rayleigh-Ritz procedure to solve, the linear algebraic equations about the unknown coefficients for coupled T-shape plates structure, cross shape plates structure and the panel-linked double-panel structure can be obtained, respectively.

$$\left[\mathbf{K_t}-\omega^2\mathbf{M_t}\right]\mathbf{E_t}=0,\quad \left[\mathbf{K_c}-\omega^2\mathbf{M_c}\right]\mathbf{E_c}=0,\quad \left[\mathbf{K_g}-\omega^2\mathbf{M_g}\right]\mathbf{E_g}=\mathbf{F_g} \quad (31)$$

$$\mathbf{E_t}=\left[\ \mathbf{W}_1^{\mathbf{T}}\quad \mathbf{U}_1^{\mathbf{T}}\quad \mathbf{V}_1^{\mathbf{T}}\quad \mathbf{W}_2^{\mathbf{T}}\quad \mathbf{U}_2^{\mathbf{T}}\quad \mathbf{V}_2^{\mathbf{T}}\right]^{\mathbf{T}} \quad (32)$$

$$\mathbf{E_c}=\left[\ \mathbf{W}_1^{\mathbf{T}}\quad \mathbf{U}_1^{\mathbf{T}}\quad \mathbf{V}_1^{\mathbf{T}}\quad \mathbf{W}_2^{\mathbf{T}}\quad \mathbf{U}_2^{\mathbf{T}}\quad \mathbf{V}_2^{\mathbf{T}}\quad \mathbf{W}_3^{\mathbf{T}}\quad \mathbf{U}_3^{\mathbf{T}}\quad \mathbf{V}_3^{\mathbf{T}}\right]^{\mathbf{T}} \quad (33)$$

$$\mathbf{E_g}=\left[\ \mathbf{W}_1^{\mathbf{T}}\quad \mathbf{U}_1^{\mathbf{T}}\quad \mathbf{V}_1^{\mathbf{T}}\quad \mathbf{W}_2^{\mathbf{T}}\quad \mathbf{U}_2^{\mathbf{T}}\quad \mathbf{V}_2^{\mathbf{T}}\quad \mathbf{W}_3^{\mathbf{T}}\quad \mathbf{U}_3^{\mathbf{T}}\quad \mathbf{V}_3^{\mathbf{T}}\right]^{\mathbf{T}} \quad (34)$$

$$\mathbf{W_1}=\left\{A_{100}...A_{1M\ N},a_{10}...a_{1M,},........,d_{10},.........d_{1M,}e_{10}...e_{1N,}.......h_{10},..........h_{1N,}\right\}^{\mathrm{T}}, \quad (35)$$

$$\mathbf{U_1}=\left\{\ B_{100}......B_{1M\ N},a_{1in0}...,a_{1inM,}b_{1in0}...,b_{1inM,}c_{1in0}...,c_{1inN,}d_{1in0}...,d_{1inN,}\ \right\}^{\mathbf{T}} \quad (36)$$

$$\mathbf{V_1}=\left\{B_{100}......,B_{1M\ N},a_{1in0}...,a_{1inM,}b_{1in0}...,b_{1inM,}c_{1in0}...,c_{1inN,}d_{1in0}...,d_{1inN,}\right\}^{\mathbf{T}} \quad (37)$$

where $\mathbf{K}$ and $\mathbf{M}$, respectively, are stiffness and mass matrices of the coupled plates structure, the natural frequencies and eigenvectors of coupled T-shape plates structure, cross shape plates structure or the panel-linked double-panel structure can be obtained by solving Eq. (31). If the eigenvectors are calculated, the dynamic response on the coupled plates can be determined by Eqs.(12) - (14).

3. NUMERICAL RESULTS AND DISCUSSIONS

3.1 Numerical results and discussions of coupled plates

3.1.1 Validation

In this section, the material parameters and dimensional parameters of the plates belonged the coupled plates structure are identical: $E = 71$ GPa , $\mu = 0.3$, $\rho = 2700$ Kg/m^3 , the thickness $h = 0.002$m and $Lx \times Ly = 1$ m$\times 1$ m. Coupling conditions are: $K_c = \infty$, $k_{c1} = \infty$, $k_{c2} = \infty$ and $k_{c3} = \infty$ Boundary conditions of plates are clamped-supported. Table 3.1 shows the first six natural frequencies of the coupled plates structure.

Table 3.1 – Natural frequencies (Hz) for the coupled coupled plates structure system

Coupled types	Mode number	M×N						FEA
		4×4	5×5	6×6	7×7	8×8	9×9	
T-shape plates structure	1	17.284	17.227	17.225	17.193	17.193	17.173	17.085
	2	33.095	33.036	33.019	33.000	32.998	32.983	32.915
	3	36.012	35.960	35.960	35.923	35.935	35.920	35.842
	4	42.630	42.228	42.211	42.007	41.989	41.888	41.389
	5	49.264	49.264	48.844	48.850	48.709	48.707	48.528
	6	51.449	51.092	51.091	51.028	51.044	51.026	50.938
cross shape plates structure	1	16.983	16.910	16.908	16.869	16.869	16.844	16.743
	2	17.777	17.777	17.775	17.775	17.775	17.775	17.770
	3	32.515	32.462	32.448	32.428	32.426	32.413	32.348
	4	35.856	35.787	35.787	35.756	35.756	35.737	35.650
	5	36.256	36.255	36.254	36.253	36.253	36.253	36.237
	6	36.257	36.256	36.255	36.253	36.254	36.254	36.238
panel-linked double-panel structure	1	16.844	16.741	16.738	16.682	16.682	16.646	16.699
	2	31.208	31.077	31.061	31.003	31.000	30.963	31.079
	3	35.785	35.690	35.690	35.645	35.645	35.616	35.965
	4	39.391	39.226	39.193	39.120	39.114	39.080	39.014
	5	44.571	43.889	43.874	43.537	43.534	43.344	42.765
	6	49.262	49.262	48.844	48.844	48.704	48.713	48.526

In this paper, it is noted that the stiffness of springs varies from extremely large (5×10^{11}) to extremely small (0), In the finite element program ANSYS, the coupling systems are meshed by SHELL63 elements ,whose size is 0.02. Figs. 3.1, 3.2 and 3.3, respectively, show some comparisons of the mode shapes for coupled T-shape plates structure, cross shape plates structure and the panel-linked double-panel structure. The corresponding mode shapes obtained from the current method agree well with that obtained from ANSYS.

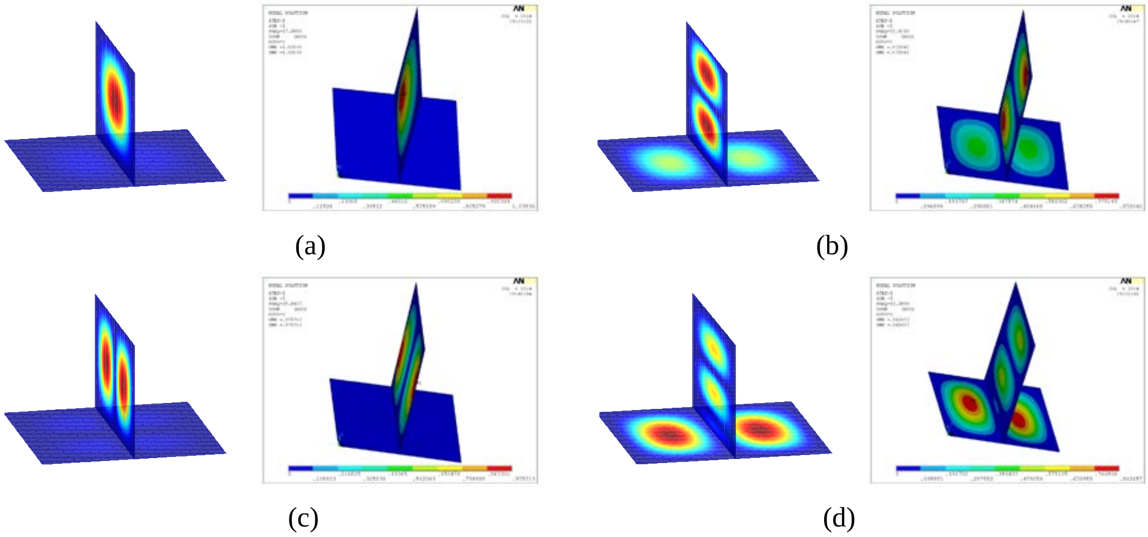

Fig. 3.1 –Mode shapes for the coupled T-shape plates structure system

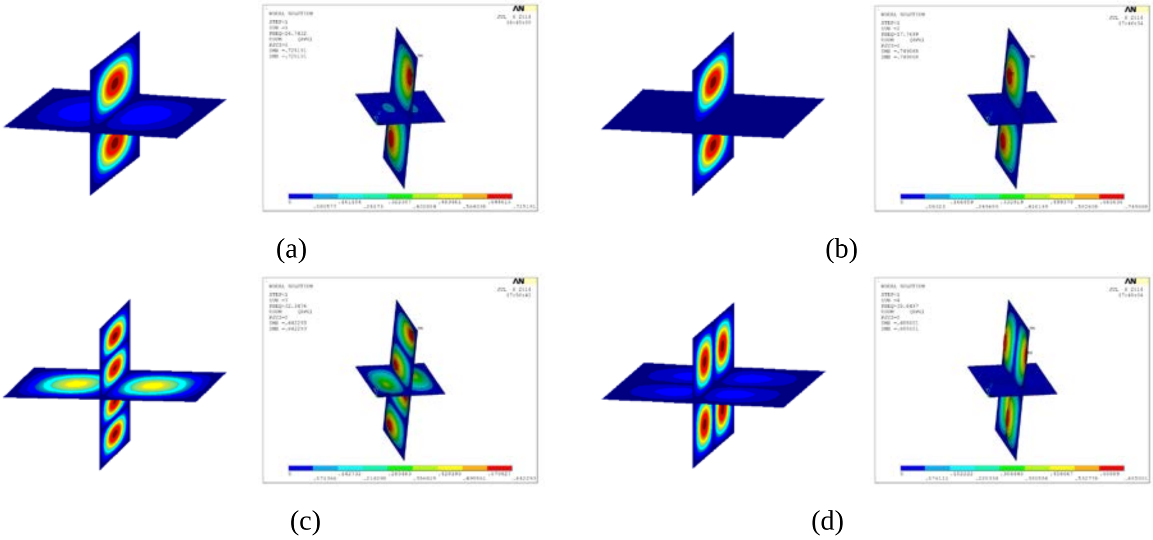

Fig. 3.2 –Mode shapes for the coupled cross shape plates

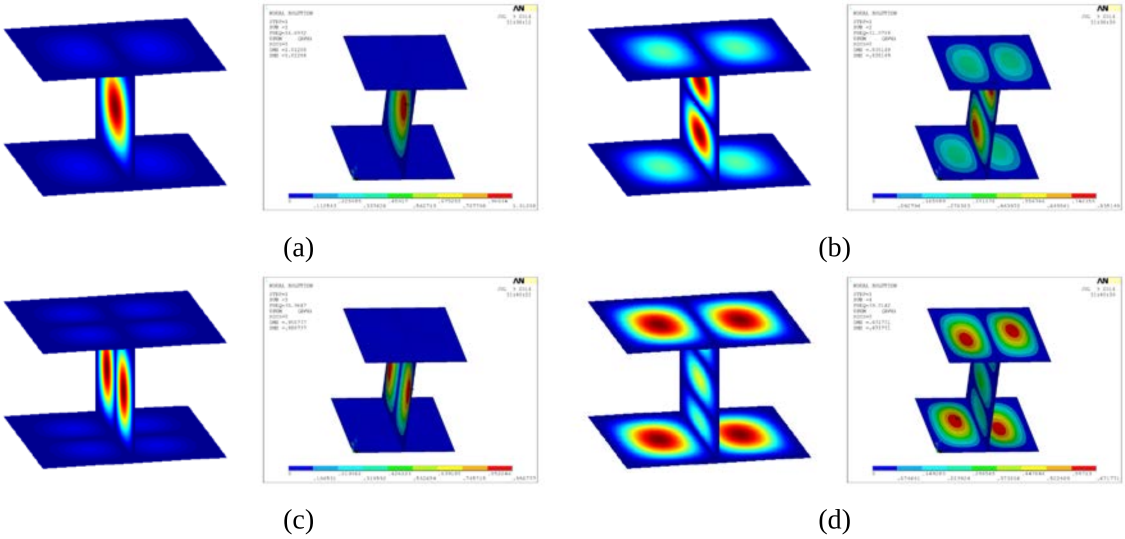

Fig. 3.3 –Mode shapes for the panel-linked double-panel structure

3.1.2 The effect of dimensional parameters of the coupled plates structure

The structural parameters play a crucial role in the vibration behavior of coupled plates structure system. The effect of some dimensional parameters on the natural frequencies for the panel-linked double-panel structure would be discussed in this section. Boundary conditions ,coupling conditions and material parameters are the same as ones described in the subsection 3.1.1. Table 3.2 and Table 3.3 show the natural frequencies for the panel-linked double-panel structures with different dimensions $\left(h_1 = 0.002\,\text{m},\ \ h_2 = 0.002\,\text{m},\ \ h_3 = 0.002\,\text{m},\ \ Lx1 \times Ly1 = 1\text{ m} \times 1\text{ m},\ \ Lx2 \times Ly2 = 1\text{ m} \times 1\text{ m},\ \ Ly3 = 1\text{ m}\right.$, various $\left. Lx3 \right)$ and different thickness $\left(h_1 = 0.002\,\text{m},\ h_2 = 0.002\,\text{m},\right.$ various h_3, $Lx1 \times Ly1 = 1\text{ m} \times 1\text{ m}$, $Lx2 \times Ly2 = 1\text{ m} \times 1\text{ m}$ and $\left. Lx3 \times Ly3 = 1\text{ m} \times 1\text{ m}\right)$, respectively. The truncation numbers are set as *M*=*N*=9.

Table 3.2 –Natural frequencies (Hz) for the panel-linked double-panel structure with various $Lx3$ (m).

$Lx3$	Mode number						
	1	2	3	4	5	6	7
0.05	44.870	48.413	48.713	49.041	59.704	63.005	63.096
0.10	42.035	46.566	48.608	48.712	57.595	61.107	63.062
0.15	40.600	44.880	48.652	48.712	56.642	59.747	63.076
0.20	39.677	43.669	48.671	48.712	56.071	58.832	63.081
0.25	38.949	42.754	48.681	48.711	55.629	58.178	63.084
0.30	38.252	42.032	48.687	48.711	55.194	57.684	63.086
0.35	37.466	41.437	48.691	48.711	54.675	57.293	63.088
0.40	36.460	40.926	48.694	48.711	53.956	56.967	63.088
0.45	35.073	40.467	48.696	48.710	52.856	56.577	56.681
0.50	33.167	40.036	48.697	48.710	50.439	51.144	56.416

Table 3.3 –Natural frequencies (Hz) for the panel-linked double-panel structure with various

various h_3,

h_3	Mode number						
	1	2	3	4	5	6	7
0.0005	4.438	9.045	9.062	13.343	16.215	16.309	20.357
0.0010	8.799	17.799	18.084	26.553	31.236	32.557	36.677
0.0015	12.915	25.421	26.976	36.576	38.987	39.091	48.701
0.0020	16.646	30.963	35.616	39.079	43.344	48.704	48.708
0.0025	20.020	34.961	41.927	43.907	48.706	48.709	48.715
0.0030	23.196	38.434	44.741	48.707	48.710	51.694	53.766
0.0035	26.317	41.618	47.139	48.708	48.710	58.168	58.320
0.0040	29.453	44.374	48.708	48.710	49.004	61.743	62.587
0.0045	32.622	46.570	48.709	48.711	50.405	63.094	63.094
0.0050	35.808	48.209	48.709	48.711	51.469	63.094	63.094

From Table 3.2 and Table 3.3, it is seen that the natural frequencies for the panel-linked double-panel structure decrease as $Lx3$ increases except for the third and four modes whose natural frequencies almost remain unchanged. The natural frequencies for the panel-linked double-panel structure increase as h_3 increases.

3.1.3 The effect of coupling conditions of the coupled plates structure

As an important factor of the coupled plates structure system, the effect of coupling conditions should be discussed. Some cases for the panel-linked double-panel structure with varied coupling conditions would be discussed to demonstrate the effect of the coupling conditions. The geometries , material parameters and boundary conditions are the same as the ones described in the subsection 3.1.1. Table 3.4 shows the natural frequencies for the panel-linked double-panel structure with different values of coupling springs $(k_{c1}=\infty$, $k_{c2}=\infty$, $k_{c3}=\infty$,various K_c, ; the coupling springs: $K_c=\infty$, various k_{c1} , $k_{c2}=\infty$, $k_{c3}=\infty$; the coupling springs: $K_c=\infty$, $k_{c1}=\infty$, various k_{c2} , $k_{c3}=\infty$ and the coupling springs: $K_c=\infty$, $k_{c1}=\infty$, $k_{c2}=\infty$, various $k_{c3})$. The truncation numbers are M=N=9.

Table 3.4 –Natural frequencies (Hz) for the panel-linked double-panel structure with one pair of stiffness-variable coupling springs as the stiffness values of the others are extremely large (5×10^{11})

Variable Stiffness	Value	Mode number							
		1	2	3	4	5	6	7	8
K_c	10^2	14.809	28.098	34.471	36.902	37.029	47.363	48.710	48.718
	10^3	16.027	30.223	35.157	38.403	40.451	48.713	48.713	48.892
	10^4	16.565	30.879	35.550	38.995	42.918	48.713	48.713	49.445
	10^5	16.637	30.954	35.609	39.071	43.300	48.713	48.713	49.513
	10^6	16.645	30.962	35.616	39.079	43.340	48.713	48.713	49.521
	10^7	16.646	30.963	35.616	39.080	43.344	48.713	48.713	49.521
k_{c1}	10^2	16.646	17.808	17.808	30.963	35.616	36.269	36.269	39.080
	10^3	16.646	18.097	18.097	30.963	35.616	36.406	36.406	39.080
	10^4	16.646	20.694	20.694	30.963	35.616	37.718	37.718	39.080
	10^5	16.646	30.963	34.123	34.123	35.616	39.079	43.344	46.783
	10^6	16.646	30.963	35.616	39.079	43.344	46.788	46.788	49.521
	10^7	16.646	30.963	35.616	39.080	43.344	48.521	48.521	49.521
k_{c2}	10^2	11.082	14.144	25.536	30.441	34.071	36.873	39.119	45.673
	10^3	11.450	14.766	25.926	30.585	34.336	36.948	39.120	45.883
	10^4	13.633	19.345	29.800	31.731	36.678	37.698	39.134	48.001
	10^5	16.118	28.752	34.561	39.055	41.536	45.592	48.713	48.713
	10^6	16.587	30.749	35.490	39.078	43.152	48.713	48.713	49.130
	10^7	16.639	30.941	35.603	39.079	43.325	48.713	48.713	49.482

It can be seen that the stiffness of coupling springs k_{c3} have very little impact on the natural frequencies for the panel-linked double-panel structure. k_{c2} and k_{c3} have lager influence on the natural frequencies than other stiffness of coupling springs for the panel-linked double-panel structure.

4. CONCLUSIONS

In this paper, the modified Fourier series method is applied to the modeling and the analysis of coupled plates of various types, which includes T-shape plates, cross shape plates and a panel-linked double-panel structure. The boundary conditions and coupling conditions are simulated by a set of elastic springs of arbitrary stiffness. All the displacements are expressed by the superposition of a two-dimensional Fourier series and several supplementary functions. Because related derivative of the displacement functions are smooth and continuous in the whole solving domain, the coefficients can be solved by using the Rayleigh-Ritz procedure based on energy principle. The reliability and accuracy of current method are verified by comparing the natural frequencies and mode shapes with ANSYS program. Some numerical examples are also conducted in order to illustrate the effect of geometry parameters and coupling conditions on the natural behavior of coupled plates. And the results show that: (a) The natural frequencies for coupled plates increase as the thickness of plate increases; (b) The natural frequencies decrease as the length of plate increases; (c) The natural frequencies are sensitive to the coupling boundaries: k_{c1} and k_{c2}.

ACKNOWLEDGEMENTS

This paper is funded by the International Exchange Program of Harbin Engineering University for Innovation-oriented Talents Cultivation.

REFERENCES

1. B. R. Mace, J. Rosenberg. The SEA of two coupled plates: an investigation into the effects of system irregularity. Journal of Sound and Vibration. 1999;212:395-415.
2. Chen Yuehua, Jin Guoyong, Du Jingtao, Liu Zhigang. Vibration characteristics and power transmission of coupled rectangular plates with elastic coupling edge and boundary restraints. Chinese journal of mechanical engineering. 2012;25(2):262-276.
3. Jingtao Du, Wen L. Li, Zhigang Liu, Tiejun Yang, Guoyong Jin. Free vibration of two elastically coupled rectangular plates with uniform elastic boundary restraints. Journal of Sound and Vibration. 2011;330(4):788–804.
4. Z. H. Wang, J. T. Xing, W. G. Price. An investigation of power flow characteristics of L- shaped plates adopting a substructure approach. Journal of Sound and Vibration. 2002;250:627-648.
5. A. N. Bercin. An assessment of the effects of in-plane vibrations on the energy flow between coupled plates. Journal of Sound and Vibration. 1996;191:661-680
6. L cheng, Y Y Li, JX Gao. Energy transmission in a mechanically-linked double-wall structure Coupled to acoustic enclosure. J Acoust Soc Am. 2005;117(6):2742-2751.
7. Yuehua Chen, Guo Yong Jin, Minggang Zhu, ZhiGang Liu, Jingtao Du,Wen L.Li. Vibration behaviors of a box-type structure built up by plates and energy transmission through the structure. Journal of Sound and Vibration. 2012;331(4):849-867.
8. N. J. Kessissoglou. Power transmission in L-shaped plates including flexural and in-plane vibration. Journal of the Acoustical Society of America. 2004;115:1157-1169.
9. J. M. Cuschieri. Structural power-flow analysis using a mobility approach of an L-shaped plate. Journal of the Acoustical Society of America. 1990;87:1159-1165.
10. J. M. Cuschieri, M. D. McCollum. In-plane and out-of-plane waves power transmission through L-plate junction using the mobility power flow approach. Journal of the Acoustical Society of America. 1996;100:857–870.
11. E. K. Dimitriadis, A. D. Pierce. Analytical solution for the power exchange between strongly coupled plates under random excitation: a test of statistical energy analysis concepts. Journal of Sound and Vibration. 1988;123:397-412.
12. S. Azimi, J. F. Hamilton, W. Soedel. The receptance method applied to the free vibration of continuous rectangular plates, Journal of Sound and Vibration. 1984;93:9-29.
13. N. H. Farag, J. Pan. On the free and forced vibration of single and coupled rectangular plates. Journal of the Acoustical Society of America. 1998;104:204-216.
14. H. S. Kim, H. J. Kang, J. S. Kim. Transmission of bending waves in inter-connected rectangular plates. Journal of the Acoustical Society of America. 1994;96:1557-1562.
15. W. L Li. Free vibrations of beams with general boundary conditions. Journal of Sound and Vibration. 2000;237:709-725.